IL NUOVO CIMENTO **42 C** (2019) 35
DOI 10.1393/ncc/i2019-19035-8

Colloquia: SoHe3 2018

Kinematics of a compression front associated with a Coronal Mass Ejection

F. Frassati([1])([2]), R. Susino([1]), S. Mancuso([1]) and A. Bemporad([1])

([1]) *INAF, Turin Astrophysical Observatory - Turin, Italy*
([2]) *University of Turin, Physics Department - Turin, Italy*

received 28 December 2018

Summary. — On 2014 November 1st a solar prominence eruption associated with a C2.7 class flare and a type II radio burst resulted in a fast partial halo Coronal Mass Ejection (CME). Images acquired in the extreme UV (EUV) by *SDO*/AIA and *PROBA-2*/SWAP, and in white light (WL) by *SOHO*/LASCO show a bright compression front expanding ahead of the CME. The main goal of this work was to infer the location and timing of the shock formation in the corona. A comparison between the starting frequency of the type II emission and the frequencies derived from the inferred coronal density distribution, allowed us to identify a region located northward of the CME as the most probable site for shock formation.

1. – Introduction

Interplanetary shocks (ISs) occur throughout the heliosphere as a result of the interaction of solar disturbances with the solar wind [1]. The study of their origin and evolution, and their associations with major solar eruptions is very important to understand the dynamics of solar eruptions and to provide a better understanding of fundamental plasma physical processes. Moreover, the Solar Energetic Particles (SEPs) accelerated by ISs constitute an important hazard for spacecraft instruments and astronauts, and affect the ionosphere causing severe geomagnetic storms and technological system disturbances.

Many open issues related to the acceleration and propagation of SEPs by CME-driven shocks are still not known (shock geometry and acceleration efficiency, nature of the seed particles accelerated, etc...), hence understanding the origin, propagation and physical properties of ISs is crucial for future developments of our capabilities of forecasting possible Space Weather effects of solar activity.

2. – Instruments and Observations

On 2014 November 1st, a prominence eruption starting around 04:00 UT resulted in a fast (leading edge speed ~ 1600 km s^{-1}) and partial-halo CME (angular width $\sim 160°$),

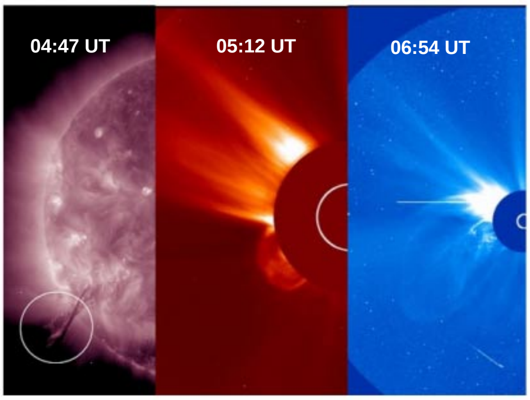

Fig. 1. – The event evolution at three different times as seen by *SDO* (left panel) and *LASCO* C2 and C3 coronographs (middle and right panels, respectively).

see Fig. 1. The eruption was associated with a type II radio burst detected by the Bruny Island Radio Spectrometer (BIRS) starting around 04:57 UT, indicating the formation and outward propagation of a CME-driven shock.

Data acquired by the Atmospheric Imaging Assembly (AIA) instrument onboard the *Solar Dynamics Observatory (SDO)* spacecraft and by the Sun Watcher using Active Pixel System detector and Image Processing (SWAP) EUV imager onboard the *Projects for Onboard Autonomy 2 (PROBA2)* have been used to study the expanding front in the lower corona. White light data recorded by the Large Angle and Spectrometric Coronagraph (LASCO) WL C2 and C3 coronagraphs on board the *Solar and Heliospheric Observatory* (*SOHO*) spacecraft have been used to study the WL front and the possible signatures of shock propagation in the higher corona from about 2.5 to 28 $R_\odot$. Radio data acquired by the Bruny Island Radio Spectrometer (BIRS) have been used as well to provide additional inputs and constraints on the shock formation time and height. More details on each instrument can be found in literature.

3. – Analysis

We developed a new technique for deriving the latitudinal distribution of the expanding front speed from a combination of AIA, SWAP, and LASCO data. In each image, the expanding front was tracked and fitted with an ellipse and only the arc of the ellipse that was common to all considered frames was used to reproduce a one-to-one correspondence between points located on different ellipses (see Fig. 2, left panel). The average front speed (computed over each front curve) is in agreement with the value from the LASCO catalogue (see Fig. 2, right panel): larger values are along the expansion direction of the front ($\sim$ 1660 km/s) and lower values towards the northern flank ($\sim$ 1490 km/s).

We built a continuous pre-event 2D map, from 1 to 28 $R_\odot$, of the electron density n_e and Alfvén speed v_A, in order to infer the condition of corona before the eruption. The pre-event electron density in AIA's FOV was calculated with the DEM inversion

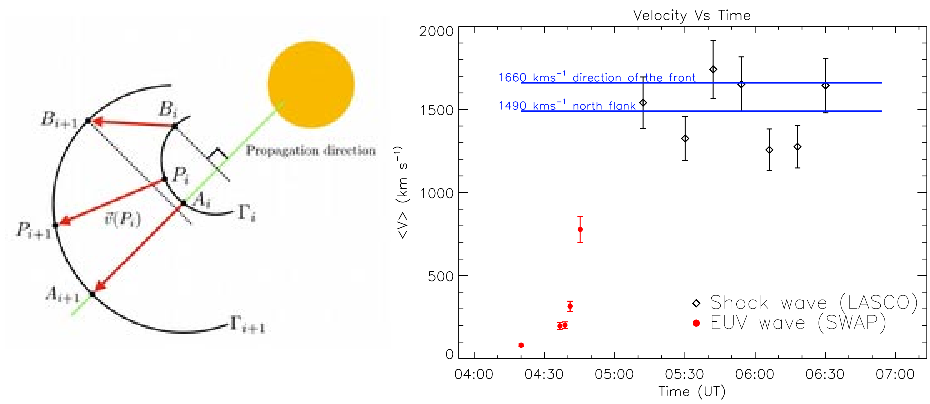

Fig. 2. – Left panel: a cartoon showing the direction of the expanding front (green line) with respect to the solar disk (yellow circle) as seen from the Sun-Earth line; the dashed black line is the perpendicular with respect to the green line passing through the ellipse center; the black solid line is the arc of the ellipse providing the kinematic parameters of the expanding front. Right panel: Average speed of the expanding front as derived from SWAP and LASCO data.

technique for AIA data developed by [2] and applied by [3], but using different temperatures. WL data were used to estimate n_e from inversion of polarized brightness (pB) measurements [4, 5]. The electron density in the region between 1.27 and 2.2 $R_\odot$, where no data are available, was derived by combining the extracted radial profiles from previous resulting maps with a linear function. To estimate the Alfvén speed, we used a theoretical model based on MHD simulations developed by Predictive Science. The 2D map of the Alfvén speed v_A was obtained from the n_e map measured from WL data and the magnetic field strength B on the plane-of-sky (POS) from MHD simulations.

To infer where the expanding front became super-Alfvénic, we compared the radial profile of the compression front speed with the Alfvén speed at three different latitudes, as shown in the left panel of Fig. 3. The radial speed derived in the northern flank (direction 'a') is higher at lower distance from the prominence origin than those along the 'b' and 'c' directions. This result suggests that the northern flank could be the location of the type II radio burst. To identify the locations of shock excitation, we compared the local plasma frequency computed where the compression front became super-Alfvénic with the starting frequency of the type II radio burst. The electron plasma frequency $\nu = 8.98\sqrt{n_e[\mathrm{cm}^{-3}]}$ kHz was derived from the electron density map and compared with the type II frequencies (starting at ~ 37 MHz). Our results (Fig. 3, right panel) show that only restricted locations (at least on the POS) along the front are compatible with the observed frequency drift and temporal evolution of the type II radio burst.

4. – Conclusion

In this work, we derived the possible location and timing of the shock formation in the corona by using EUV, WL and Radio observations. The presence of a type II radio burst is a clear signature of a shock excited out of the field of view covered by *SDO*/AIA. We derived the latitudinal speed distribution of the expanding front and compared it with

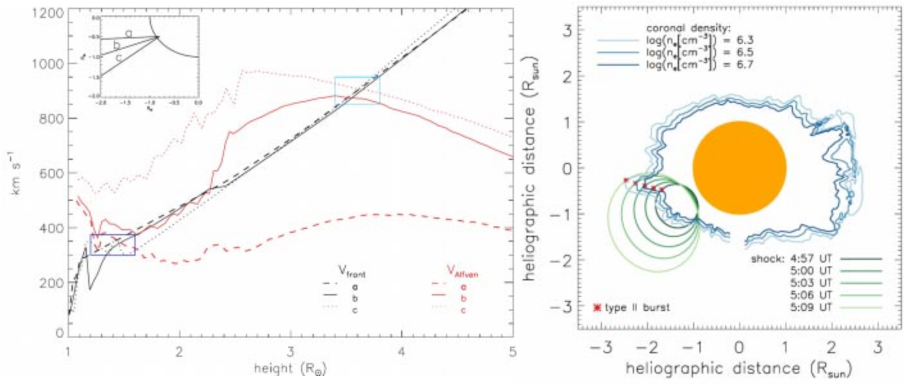

Fig. 3. – Left panel: comparison between the Alfvén speed (red) and the compression front speed (black) as a function of altitude at three different latitudes ('a', 'b', and 'c', see box at the top). The two blue boxes localize the height, with respect to the origin of the prominence on the limb, where the compression front speed exceeds Alfvén speed. Right panel: a cartoon showing the expanding shock surfaces (green ellipses) at 5 different times. The red stars mark the most probable location of the metric type II burst along the shock surface.

the Alfvén speed: the northern flank became super-Alfvénic at a lower distance from the solar limb than the other regions. We derived the coronal electron density and thus the plasma frequency to compare it with the frequency of the type II radio burst detected by BIRS: only restricted locations on the northern flank of the front are compatible with the observed frequency drift and temporal evolution of the type II radio burst.

This is in qualitative agreement with the presence of nearby coronal loop structures located northward of the eruption source region (as seen by the AIA images, Fig. 1, left panel) and of a faint North-East coronal streamer complex (as seen by the SOHO/LASCO-C2 coronagraph, Fig. 1, middle panel). Hence, the northward part of the EUV front was likely interacting with denser, nearby features in the lower corona, becoming the most probable location for the type II radio burst.

* * *

We are grateful to the *SOHO*, *SDO*, *PROBA2*, and BIRS teams for making their data available to us. F.F. acknowledges support from INAF Ph.D. grant and from the PROBA2 Guest Investigator Program.

REFERENCES

[1] Richter A. K., *et al.*, *AGU, Washington, D. C.*, **35** (1985) 33-50.
[2] Aschwanden M. J., *et al.*, *SoPh*, **283** (2013) 5.
[3] Frassati F., *et al.*, *Ap&SS*, **362** (2017) 194.
[4] van de Hulst H. C., *BAN*, **11** (1950) 135.
[5] Koutchmy S., and Lamy P. L., *Ap&SSL Conf. Ser.*, **119** (1985) 63-74.